

การเตรียมฟิล์มบางคอปเปอร์อินเดียมแกลเลียมไดซัลไฟด์สำหรับ
เซลล์แสงอาทิตย์ประสิทธิภาพสูง

นายชาญวิทย์ จิตยุทธการ

วิทยานิพนธ์นี้เป็นส่วนหนึ่งของการศึกษาตามหลักสูตรปริญญาวิทยาศาสตรดุษฎีบัณฑิต

สาขาวิชาฟิสิกส์ ภาควิชาฟิสิกส์

คณะวิทยาศาสตร์ จุฬาลงกรณ์มหาวิทยาลัย

ปีการศึกษา 2547

ISBN 974-17-6039-6

ลิขสิทธิ์ของจุฬาลงกรณ์มหาวิทยาลัย

**FABRICATION OF Cu(In,Ga)Se_2 THIN FILMS FOR HIGH EFFICIENCY
SOLAR CELLS**

Mr. Chanwit Chityuttakan

**A Dissertation Submitted in Partial Fulfillment of the Requirements
for the Degree of Doctor of Philosophy in Physics**

Department of Physics

Faculty of Science


Chulalongkorn University

Academic year 2004


ISBN 974-17-6039-6


Thesis Title Fabrication of Cu(In,Ga)Se₂ Thin Films for High Efficiency Solar Cells
By Mr. Chanwit Chityuttakan
Field of Study Physics
Thesis Advisor Assistant Professor Kajornyod Yoodee, Ph.D.
Thesis Co-advisor Assistant Professor Somphong Chatraphorn


Accepted by the Faculty of Science, Chulalongkorn University in Partial Fulfillment of the Requirements of Degree of Doctor of Philosophy



..... Dean of the Faculty of Science
(Professor Piamsak Menasveta, Ph.D.)

Thesis Committee



..... Chairman
(Associate Professor Prapaipan Chantikul, Ph.D.)


..... Thesis Advisor
(Assistant Professor Kajornyod Yoodee, Ph.D.)


..... Thesis Co-advisor
(Assistant Professor Somphong Chatraphorn)


..... Member
(Associate Professor Anantasin Techagumpuch, Ph.D.)


..... Member
(Associate Professor Wichit Sritrakool, Ph.D.)


..... Member
(Assistant Professor Vittaya Amornkitbamrung, Ph.D.)

ชาญวิทย์ จิตยุทธการ : การเตรียมฟิล์มบางคอปเปอร์อินเดียมแกเลียมไคซีลีไนด์สำหรับเซลล์แสงอาทิตย์ประสิทธิภาพสูง. (FABRICATION OF Cu(In,Ga)Se₂ THIN FILMS FOR HIGH EFFICIENCY SOLAR CELLS) อ. ที่ปรึกษา : ผศ. ดร. ขจรยศ อยู่ดี, ผศ. สมพงษ์ ฉัตรภากรณ์, 146 หน้า. ISBN 974-17-6039-6.

ได้ออกแบบและสร้างระบบเตรียมฟิล์มบางคอปเปอร์อินเดียมแกเลียมไคซีลีไนด์ Cu(In,Ga)Se₂ (CIGS) สำหรับประดิษฐ์เซลล์แสงอาทิตย์ประสิทธิภาพสูงตามโครงสร้าง (Ni)Al/ZnO(AI)/CdS/CIGS/Mo/SLG ซึ่งฟิล์มบาง CIGS มีความหนาประมาณ 2 ไมครอนถูกเตรียมบนแผ่นรองรับที่อุณหภูมิคงที่ รวมถึงการศึกษาผลกระทบของอุณหภูมิมบนแผ่นรองรับที่ใช้ต่างกันคือ 475, 500, 525 และ 550°C ต่อฟิล์ม CIGS สำหรับวิธีการเตรียมฟิล์ม CIGS จะใช้วิธีการระเหยร่วมกันจากแหล่งระเหยธาตุทั้งสี่แหล่งร่วมกับเทคนิคการตรวจวัดสัญญาณ ณ เวลาจริง เพื่อใช้ควบคุมกระบวนการและที่จุดสิ้นสุด (EPD) ในการทดลองเตรียมฟิล์มบาง CIGS ได้ใช้โปรไฟล์อุณหภูมิ 2 แบบโดย แบบแรก Cu-Rich-Off (CURO) process เริ่มต้นปลูกด้วย Cu-rich stage ให้ฟิล์มที่มีสัดส่วนอะตอมของ [Cu]/([In]+[Ga]) มากกว่าหนึ่ง ($y > 1$) แล้วต่อด้วย Cu-poor stage จนกระทั่งได้เนื้อฟิล์มทั้งหมดที่มีค่า $y < 1$ และหยุดปลูกที่ค่า $y \approx 0.9$ จากผลการวิเคราะห์ฟิล์มด้วยวิธี XRD และ SEM แสดงว่าการปลูกแบบนี้ให้ฟิล์มที่มีโครงสร้างแบบซาลโคไฟไรท์ โครงผลึกส่วนมากหันระนาบ (112) ขนานกับระนาบของแผ่นรองรับ มีเกรนเป็นแท่งใหญ่ และมีรูขุมระมีรอยแตกแยกเล็ก เมื่อประดิษฐ์เป็นเซลล์แสงอาทิตย์แล้ววัดลักษณะส่อของกระแสและความต่างศักย์ไฟฟ้า (I-V) และประสิทธิภาพเชิงควอนตัม (QE) พบว่ามีประสิทธิภาพสูงถึง 14% ส่วนแบบที่สอง Cu-Poor-Rich-Off (CUPRO) process เริ่มต้นปลูกด้วย Cu-poor stage ด้วยค่า $y < 1$ แล้วต่อด้วย Cu-rich stage จนกระทั่งได้เนื้อฟิล์มทั้งหมดที่มีค่า $y > 1$ แล้วต่อด้วย Cu-poor stage จนกระทั่งได้เนื้อฟิล์มทั้งหมดที่มีค่า $y < 1$ โดยหยุดปลูกที่ค่าเดียวกัน ($y \approx 0.9$) จากผลการวิเคราะห์พบว่า ฟิล์มมีโครงสร้างแบบซาลโคไฟไรท์ โครงผลึกหันระนาบ (220)(204) ขนานกับระนาบของแผ่นรองรับมากขึ้น มีเกรนเป็นแท่ง และมีรอยแตกแยกไม่ลึกจากขอบบนของเกรน เมื่อประดิษฐ์เป็นเซลล์แสงอาทิตย์แล้วได้ประสิทธิภาพสูงในระดับ 15% ในงานวิจัยได้เสนอแบบจำลองการเกิดของฟิล์มที่เตรียมจากทั้งสองวิธีซึ่งสอดคล้องกันคือ การมี Cu_xSe ส่วนเกินแยกตัวอยู่ที่ผิวฟิล์มและระหว่างขอบเกรนของฟิล์ม Cu-rich ซึ่งเป็นที่มาของรอยแตกแยกจากการเปลี่ยนแปลงของ Cu_xSe ไปเป็น CIGS อีกทั้งมี recrystallization เกิดขึ้นในการเตรียมฟิล์มแบบ CUPRO process

ภาควิชา ฟิสิกส์
สาขาวิชา ฟิสิกส์
ปีการศึกษา 2547

ลายมือชื่อนิสิต.....
ลายมือชื่ออาจารย์ที่ปรึกษา.....
ลายมือชื่ออาจารย์ที่ปรึกษาร่วม.....

4273843023 : MAJOR PHYSICS

KEY WORD: SOLAR CELL / FABRICATION / IN SITU MONITORING / HIGH EFFICIENCY/ CIGS

CHANWIT CHITYUTTAKAN: FABRICATION OF Cu(In,Ga)Se_2 THIN FILMS FOR HIGH EFFICIENCY SOLAR CELLS. DISSERTATION ADVISOR: ASST. PROF. KAJORN YOD YOODER, PH.D. DISSERTATION COADVISOR: ASST. PROF. SOMPHONG CHATRAPHORN. 146 pp. ISBN 974-17-6039-6.

A deposition system for fabrication of high efficiency Cu(In,Ga)Se_2 (CIGS) thin films was designed and constructed. The structure of the CIGS solar cells consists of five different layers of materials, $(\text{Ni})\text{Al/ZnO(Al)/CdS/CIGS/Mo/SLG}$, where the SLG is the soda-lime-glass substrate. The CIGS absorber layers of approximately $2 \mu\text{m}$ thick were co-evaporated from four elemental sources onto the Mo/SLG substrates with constant substrate temperatures. The temperature effect on CIGS films was also studied using different substrate temperatures of 475, 500, 525 and 550°C . The *in situ* monitoring technique was employed for process control and end point detection (EPD). Two temperature profiles were performed in the CIGS deposition process. First, Cu-Rich-Off (CURO) process was started with the Cu-rich stage such that the atomic ratio $[\text{Cu}]/([\text{In}]+[\text{Ga}])$ was greater than 1 ($y > 1$), then followed by the Cu-poor stage until $y < 1$ was reached, and the process was finished at $y \approx 0.9$. Film analysis results using XRD and SEM showed that these films were typically (112) oriented chalcopyrite with large columnar grains and rough surfaces with deep crevices. From the current-voltage (I-V) and the quantum efficiency (QE) measurements, the CIGS thin film solar cells fabricated with this process yielded efficiencies up to 14%. In the second profile, Cu-Poor-Rich-Off (CUPRO) process started with the Cu-poor stage, $y < 1$, followed by the Cu-rich stage until $y > 1$, then finished with the Cu-poor stage at the same value ($y \approx 0.9$). The results showed that these films were weakly (220)(204) oriented chalcopyrite with columnar grains and smooth surfaces with shallow crevices. These CIGS thin films solar cells showed their efficiencies at the level of 15%. The proposed growth models for these two processes implicated that the excess Cu_xSe in the Cu-rich films segregated and presented at the surfaces of the films and between the grain boundaries. The crevices resulted from the conversion of the Cu_xSe to CIGS. Furthermore, recrystallization was found to occur in the CUPRO growth process.

Department	Physics	Student's signature.....	<i>Chanwit Chityuttakan</i>
Field of study	Physics	Advisor's signature.....	<i>Kajorn yod Yooder</i>
Academic year	2004	Co-advisor's signature.....	<i>Somphong Chatraphorn</i>

ACKNOWLEDGEMENTS

I would like to express my sincere gratitude to the following persons:

-My supervisors, Assist. Prof. Dr. Kajornyod Yoodee and Assist. Prof. Somphong Chatraporn for invaluable discussions, scientific skill, guidance and encouragement throughout the work on this thesis.

-Dr. John Kessler for many helpful discussions, new and interesting ideas, scientific knowledge, technical supports, encouragement and friendship.

-Assoc. Prof. Dr. Prapaipan Chantikul, Assoc. Prof. Dr. Wichit Sritrakool, Assoc. Prof. Dr. Anantasin Techagumpuch, Assist. Prof. Dr. Vittaya Amornkitbumrung for their reading and criticizing the manuscript.

-Prof. Lars Stolt, for research collaboration, and I would also like to thank other colleagues and students at the Ångstrom Solar Center (ÅSC), Uppsala University, Sweden for many discussions and friendly during the whole period of working at ÅSC.

-I would like to thanks Dr. Sojiphong Chatraphorn and Dr. Chatchai Srinitiworrawong for their helps.

-I acknowledge the financial support from Chulalongkorn University, Thailand, for the scholarship for my doctoral study, MTEC for the equipments and financial support. I also acknowledge the ISP; Dr. Lennart Hasselgren for the financial support and giving me the opportunity to work at ÅSC.

-Finally, I would like to thank Miss Panita Chinvetkitvanich for her help and encouragement during the period of my doctoral studies. I would also like to express my gratitude to my parents and my brothers for their encouragement and everything they have done for me.

TABLE OF CONTENTS

ABSTRACT IN THAI.....	iv
ABSTRACT IN ENGLISH	v
ACKNOWLEDGEMENTS	vi
TABLE OF CONTENTS	vii
LIST OF FIGURES	x
LIST OF TABLES	xvi
CHAPTER I INTRODUCTION	1
1.1 Overview.....	1
1.2 Copper Indium Diselenide and Related Materials for Thin Film Solar Cells	4
1.3 Outline of the Research	7
CHAPTER II MATERIAL PROPERTIES OF CIS-BASED THIN FILMS AND SOLAR CELLS.....	10
2.1 Material Properties of CIS-Based Thin Films	10
2.1.1 The Cu-In-Se Material System.....	10
2.1.2 Crystal Structure of CuInSe ₂	12
2.1.3 Defect of CuInSe ₂	14
2.2 Physical Principle of the Solar Cell	17
2.2.1 Solar Spectrum	17
2.2.2 Electrical Properties of Solar Cells.....	19
CHAPTER III THE DEPOSITION SYSTEM FOR CIGS THIN FILMS	24
3.1 Evaporation Process	24
3.1.1 Introduction.	24
3.1.2 Model of Film Growth in Evaporation Process	26

3.1.3	Basic Theory and Mechanisms	28
3.2	The CIGS Deposition System.....	34
3.2.1	Vacuum Chamber and Pumping System	36
3.2.2	Graphite Heater and Substrate Holder.....	38
3.2.3	Evaporation Sources (Cu, In, Ga and Se).....	39
3.2.4	Shutter and Radiation Shield.....	42
3.2.5	Source Calibration	42
3.2.6	Pyrometer	47
CHAPTER IV	EXPERIMENTAL PROCEDURE	49
4.1	Fabrication of CIGS Thin Film Solar Cells.....	49
4.2	Growth of CIGS Thin Films by PVD Technique	53
4.2.1	General Calculation for CIGS Deposition Process	53
4.2.2	The Two-Stage or Cu-Rich-Off (CURO) Process	57
4.2.3	The Modified Two-Stage or Cu-Poor-Rich-Off (CUPRO) Process	60
4.3	Characterization of CIGS Thin Films	63
4.4	Characterization of Cell Performance	66
4.4.1	Current-Voltage (I-V) Measurement	66
4.4.2	Quantum Efficiency (QE) Measurement	68
CHAPTER V	RESULTS AND DISCUSSION.....	71
5.1	Results and Discussion of the CIGS Films Grown by CURO Process and the Cell Performances.....	72
5.1.1	<i>in situ</i> Monitoring of the Growth of CIGS thin Films: EPD based T_{pyro} , T_{sub} and OP	72
5.1.2	Crystal Structure of the Films Grown by CURO Process	76
5.1.3	Morphology of the Films Grown by CURO Process	79
5.1.4	Growth Model for CURO Process	82
5.1.5	Cell Performances of the Films Grown by CURO Process..	87

5.1.6	Conclusions: CURO Process.....	90
5.2	Results and Discussion of the CIGS Films Grown by CUPRO Process and Cell Performances	91
5.2.1	Film Growth by CUPRO Process.....	91
5.2.2	Effect on Film Orientation: (112) vs. (220)(204).....	94
5.2.3	Effect on Film Morphology	98
5.2.4	Effect on Substrate Temperatures	102
5.2.5	Cell Performances of the Films Grown by CUPRO Process.....	105
5.2.6	Five-Stage Growth Model.....	110
5.2.7	Conclusions: CUPRO Process	114
CHAPTER VI CONCLUSIONS AND SUGGESTIONS.....		115
REFERENCES		119
APPENDICES		126
APPENDIX A LIST OF ABBREVIATIONS		127
APPENDIX B LIST OF PUBLICATIONS		129
CURRICULUM VITAE		130

LIST OF FIGURES

Figure	Page
1.1 The evolution of efficiencies of the best thin film solar cells for a-Si, CIGS and CdTe	2
1.2 Absorption coefficient spectrum of CuInSe ₂ compared with that of other photovoltaic semiconductors.....	4
2.1 Phase diagram along the Cu ₂ Se-In ₂ Se ₃ pseudobinary section of the Cu-In-Se material system	11
2.2 Schematic representation of CuInSe ₂ chalcopyrite structure (a) conventional unit cell, (b) cation-centered first coordinate shell (c) anion-centered first coordinate shell showing bond lengths $d_{\text{Cu-Se}}$ and $d_{\text{In-Se}}$	13
2.3 Lattice constants a and $c/2$ of the CuInSe ₂ -CuGaSe ₂ alloy system.....	14
2.4 Spectral energy distribution for space (AM0), Central Europe (AM1.5), and the theoretical curve for a black body at about 5800K (dashed line). The upper scale in the figure shows the energy of the photons corresponding to the wavelength in the lower scale	17
2.5 Ideal solar cell efficiency as a function of the band gap energy for the spectral distribution AM0 and AM1.5 with a power density of 1 sun, and for AM1.5 with 1000 suns (= 844kW/m ²).....	18
2.6 Band diagram of a p-n junction solar cell under illumination.....	19

2.7	(a) the equivalent circuit of solar cells, (b) I-V characteristic curve of a solar cell in dark and under illumination. The grey rectangle defines the point of maximum output power P_{max} which is important for solar cell operation	21
2.8	I-V curve for an actual CIGS thin film solar cell, with the solar cell parameters	23
3.1	Schematic diagram of an evaporation system using electron beam heating	25
3.2	Schematic diagram of a simplified sputtering system: DC and RF	26
3.3	The three steps in film deposition for PVD process	27
3.4	Evaporation from (a) a point source, (b) a surface source	29
3.5	Geometry of h and x , vertical and horizontal substrate distances, respectively	32
3.6	(a) Photograph of the CIGS deposition system at SPRL, (b) Schematic diagram of the multi-source co-evaporation system with the <i>in situ</i> monitoring: heating output power, pyrometer, thermocouples	35
3.7	Photograph of the vacuum chamber.....	37
3.8	Schematic diagram of the vacuum pumping system.....	37
3.9	Photographs of the graphite heater and the substrate holder.....	38
3.10	Schematic drawing of the graphite heater and the substrate	39
3.11	Photographs of the evaporation sources for Cu, In, Ga and Se.....	40

3.12	Photograph of the structure of evaporation sources.....	41
3.13	Photograph of the shutter and radiation shield	42
3.14	Photograph of the optical transmission measurement set-up for the thickness distribution of film on the substrate.....	43
3.15	The thickness distribution of Cu film on the large area of glass substrates.....	43
3.16	Photograph of the quartz crystal monitor at the center of substrate	44
3.17	The plots of $\ln(r)$ versus $1/T$ for (a) the Cu source, (b) the In source, (c) the Ga source and (d) the Se source	46
3.18	Photographs of the pyrometer	47
4.1	Schematic diagram (not to scale) of the CIGS thin film solar cell structure	50
4.2	Schematic diagram of the CIGS fabrication process	52
4.3	Photograph of the CIGS thin film solar cells (8 rows x 5 columns) fabricated at SPRL.....	53
4.4	Temperature profiles of sources and substrate for CIGS film deposition by CURO process, Y being a ratio of Cu flux; $\Phi_{Cu}/(\Phi_{In}+\Phi_{Ga})$	57
4.5	Evolution of film compositions, $y(t)$ and $x(t)$ during the deposition process of temperature profiles in Fig. 4.4	58
4.6	Temperature profiles of sources and substrate for CIGS film deposition by CUPRO process. Y being a ratio of Cu flux.....	61

4.7	Evolution of film compositions, $y(t)$ and $x(t)$ of the temperature profiles in Fig. 4.6.....	62
4.8	X-ray spectrum of a CIGS thin film.....	64
4.9	(a) Photograph of the I-V measurement system, (b) Schematic diagram of the I-V measurement system	67
4.10	Schematic diagram of QE measurement set-up.....	68
4.11	Typical wavelength resolved quantum efficiency plot of a CIGS solar cell, the solar spectrum (AM1.5) also shown in the figure	69
5.1	Typical temperature profiles of Cu, In, Ga sources and calculated content of Cu (y_{cal}) of the growing film by CURO process	72
5.2	The <i>in situ</i> monitoring signals of the temperatures profiles in Fig 5.1	73
5.3	XRD spectra of the films R, S and P represent the evolution of CURO growth at the end of states II, III and IV, respectively	76
5.4	SEM micrographs (surface) of the films R, S and P represent the evolution of CURO growth at the end of states II, III and IV, respectively	79
5.5	SEM micrograph (cross-section) of the film S at $y \approx 0.9$ (EPD) as shown in Fig. 5.1.....	81
5.6	Growth model for Cu-rich $\text{Cu}(\text{In,Ga})\text{Se}_2$ by two-stage or CURO process with the presence of a copper chalcogenide phase.....	84
5.7	Growth model for the conversion of Cu_xSe into $\text{Cu}(\text{In,Ga})\text{Se}_2$ by exposure to an (In,Ga)-rich vapor trail	84

5.8	Pictorial representation of the Cu_xSe /surface modification process. (a) Cu-rich, (b) nearly stoichiometric, (c) Cu-poor	86
5.9	Growth model for the CURO process	87
5.10	Typical cell performances, V_{oc} , J_{sc} , FF and the efficiency for a sample grown by CURO process at $T_{sub} \approx 510^\circ\text{C}$, as a function of position, for a typical $3 \times 5 \text{ cm}^2$ substrate. The sample is divided into 16 cells (2 rows and 8 columns) of 0.5 cm^2 each.....	88
5.11	I-V curve of the best CIGS solar cell using the <i>in situ</i> monitoring in the typical two-stage or CURO process at $T_{sub} \approx 510^\circ\text{C}$	90
5.12	QE of the best CIGS solar cell using the <i>in situ</i> monitoring in the typical two-stage or CURO process at $T_{sub} \approx 510^\circ\text{C}$ as shown in Fig. 5.11	91
5.13	(a) Typical temperature profiles of Cu, In and Ga sources by CUPRO process. (b) The <i>in situ</i> monitoring of output power signal of the deposition process. (c) The values of Cu content of the growing film from both calculation and estimation.....	92
5.14	Six different film growths (A-F) produced from the different $y(t)$ evolutions	95
5.15	Evolution of the selective XRD results from (112), (220)(204) and (116)(312) peaks for the films shown in Fig. 5.14.....	96
5.16	SEM micrographs (cross-section about 10° tilt) of the films shown in Fig. 5.14 (except film F). Top row: films A and B, uniform fluxes at $y = 0.90$ and $y = 0.75$. Bottom row: films C-E, evolution of the CUPRO growth.....	99

5.17	TEM micrographs (cross-section) of the films shown in Fig. 5.14 (except film A and film F). Top row: films C to B, evolution of the uniform flux growth at $y = 0.75$. Bottom row: films C-E, evolution of the CUPRO growth.....	101
5.18	Evolution of the selective XRD results from (112), (220)(204) and (116)(312) peaks for the films grown at different substrate temperatures	103
5.19	SEM micrographs (cross-section about 10° tilt) of the four CUPRO grown Cu(In,Ga)Se ₂ films at different substrate temperatures of 475, 500, 525, and 550 °C	104
5.20	Typical cell performances for a sample grown by CUPRO process at $T_{\text{sub}} \approx 500^\circ\text{C}$, as a function of position, for a typical 5x5 cm ² substrate. The sample is divided into 32 cells (4 rows of 8 columns) of 0.5 cm ² each.....	106
5.21	Current-voltage characteristics of the best cells grown by CUPRO process for the four studied substrate temperatures	109
5.22	Quantum efficiencies of the best cells grown by CUPRO process for the four studied substrate temperatures shown in Fig. 5.21	109
5.23	Five-stage growth model	113

LIST OF TABLES

Table	Page
2.1	Majority defect pairs in CuInSe ₂ under the condition $\Delta m < 0$ 16
2.2	Formation energies of intrinsic defects in CuInSe ₂ 16
3.1	Properties of selective materials for the source components..... 41
4.1	Density and mass per mole values of the materials 54
4.2	α parameter of the elements..... 55
4.3	Required data for the deposition process..... 60
4.4	Calculated values using the required data in Table 4.3..... 60
5.1	Calculated values of a, c, c/a and z from the XRD patterns of the films R, S and P shown in Fig. 5.3 and JCPDS for CuIn _{1-x} Ga _x Se ₂ where $x = 0, 0.25$ and 0.4 78
5.2	Statistical values of the current-voltage parameters for the sample as shown in Fig. 5.10 89
5.3	Orientation ratios $z = I(112)/I(220)(204)$ for the films shown in Fig. 5.15 97
5.4	Orientation ratios $z = I(112)/I(220)(204)$ for the films grown at different substrate temperatures 103
5.5	Statistical values of the current-voltage parameters for the sample as shown in Fig. 5.20 107
5.6	Cell performances of the best cells grown by CUPRO process for the four studied substrate temperatures..... 108